Complete set of material constants of single domain (K, Na)(Nb, Ta)O_3 single crystal and their orientation dependence

Limei Zheng,[1] Shiyang Li,[2] Shijing Sang,[1] Junjun Wang,[1] Xiaoqing Huo,[1] Rui Wang,[3] Zhongyuan Yuan,[1] and Wenwu Cao[1,4,a)]
[1]*Condensed Matter Science and Technology Institute, Harbin Institute of Technology, Harbin 150080, China*
[2]*Department of Instrument Science and Engineering, Shanghai Jiao Tong University, Shanghai 200240, China*
[3]*Department of Chemistry, Harbin Institute of Technology, Harbin 150080, China*
[4]*Department of Mathematics and Materials Research Institute, The Pennsylvania State University, University Park, Pennsylvania 16802, USA*

(Received 16 October 2014; accepted 12 November 2014; published online 25 November 2014)

A self-consistent complete set of dielectric, piezoelectric, and elastic constants for single domain Ta modified (K, Na)NbO_3 (KNN) crystal was determined. This full set constant for single domain KNN-based crystals allowed the prediction of orientation dependence of the longitudinal dielectric, piezoelectric, elastic coefficients, and electromechanical coupling factors. The maximum piezoelectric and electromechanical properties were found to exist near $[001]_C$. In addition, material constants of $[001]_C$ poled domain engineered single crystal with 4 mm symmetry were experimentally measured and compared with the calculated values. Based on this, extrinsic contribution to the piezoelectricity was estimated to be ~20%. © *2014 AIP Publishing LLC*.
[http://dx.doi.org/10.1063/1.4902548]

Lead-free piezoelectric materials have been extensively studied in the last decade because most of currently used piezoelectric materials are Pb-based, which are environmentally hazardous. Among all lead-free piezoelectric materials reported so far, the (K, Na)NbO_3 (KNN) system has drawn much attention due to its high Curie temperature and excellent piezoelectric properties,[1–4] especially after the breakthrough made in KNN-based ceramics by Yasuyoshi *et al.* in 2004.[5] Great improvement for KNN-based ceramics has been achieved in recent years both in preparation techniques and piezoelectric performance.[6–8] By contrast, study on the KNN-based single crystals is limited because of the difficulty in growing large size KNN-based single crystals.[9–13]

In our previous work, Ta modified KNN based single crystal (abbreviated as KNNT) with large size and high quality had been grown by the top-seeded solution growth (TSSG) technique, and the complete sets of elastic, dielectric, and piezoelectric constants for the $[001]_C$ poled multidomain samples were reported.[14]

It is known that piezoelectric properties come from both intrinsic and extrinsic contributions; the intrinsic contribution refers to the effect of crystal anisotropy of single domain state, while the extrinsic contribution comes from the motion of domain walls. In order to gain further insight into the nature of piezoelectric activity in $[001]_C$ poled domain engineered single crystals, it is necessary to delineate these two types of contributions.[15–17] One cannot evaluate the intrinsic and extrinsic contributions qualitatively without a complete data set of the single domain state. Using the single domain data, one could analyze the orientation dependence of functional properties in order to get the optimum cut for particular applications, and also analyze the intrinsic and extrinsic contributions of the piezoelectric properties.

In this study, a large size Ta modified KNN single crystal (abbreviated as KNNT-2, to distinguish it from the KNNT crystal reported previously[14]) was grown by the top-seeded solution growth technique. The single-domain state was realized using a 2-step poling procedure by applying a field along $[011]_C$. A full set of property matrix for the single domain KNNT-2 single crystal was measured. Based on these single domain data, orientation dependence of dielectric, piezoelectric, elastic, and electromechanical coupling properties were calculated, and the extrinsic contributions to the piezoelectric properties were estimated by comparing the calculated and measured values of the $[001]_C$ poled samples.

The KNNT-2 single crystal was grown by the top-seeded solution growth method. High purity (99.99%) Na_2CO_3, K_2CO_3, Ta_2O_5, and Nb_2O_5 were chosen as raw materials. The growth procedure is similar to the KNNT crystal reported previously.[14]

For the $[011]_C$ poled samples, the macroscopic symmetry is the same as the crystal symmetry with the orthorhombic point group *mm*2. There are total 17 independent material constants: nine elastic constants, five piezoelectric constants, and three dielectric constants. The *z*-axis is along the poling direction $[011]_C$, with *x* and *y* axes along the pseudo-cubic crystallographic directions $[0\bar{1}1]_C$ and $[100]_C$, respectively. All samples were oriented by a Laue x-ray machine with an accuracy of ±0.5°, and designed with aspect ratios according to the IEEE standards. Vacuum sputtered gold was applied to the desired surfaces as electrodes. In order to achieve single-domain state, two-step poling technique was adopted.[18] In the 1st step, samples were poled at a temperature slightly above the orthorhombic-tetragonal phase transition temperature, e.g., around 100 °C, under the electric field of 1 kV/cm for 3 min, then slowly cooled down to 40 °C with the electric field on. Finally, the sample was naturally cooled to room temperature after removing the field. In the 2nd step, a DC field of 20 kV/cm was applied to

a)Author to whom correspondence should be addressed. Electronic mail: dzk@psu.edu. Tel.: 1 (814) 865-4101. Fax: 1 (814) 865-2326.

the samples at room temperature for 10 min. The $[001]_C$ oriented multidomain samples were directly poled under a DC electric field of 35 kV/cm at room temperature for 10 min. Domain configuration was studied by using polarizing light microscopy (PLM). The dielectric constant was determined using an HP 4284A multi-frequency LCR meter. The resonance and antiresonance frequencies were measured using an HP 4294A impedance-phase analyzer. The piezoelectric coefficients and electromechanical coupling factors were determined by resonance and antiresonance frequencies, following the IEEE standards. Combined resonance and pulse-echo ultrasonic method were used to determine the complete sets of elastic, dielectric, and piezoelectric constants with the strategy of over determination. Furthermore, to guarantee the self-consistency and accuracy of the full set physical properties, the inverse impedance spectroscopy method was used to further check the data sets.[19–22]

Fig. 1(a) shows a photograph of the as-grown KNNT-2 single crystal. The dimensions of the crystal are $21 \times 21 \times 8\,mm^3$, much larger than previously grown KNNT crystals. Some cracks along $\{100\}_C$ plans can be observed due to the large strain formed at the cubic-tetragonal phase transition temperature T_C and tetragonal-orthorhombic phase transition temperature $T_{O\text{-}T}$ during the cooling process.

In order to verify the composition homogeneity, local composition of different parts in the cross section of KNNT-2 single crystal were checked by Energy Dispersive Spectrometry (EDS). No evident compositional variation was found along the radial direction. However, slight gradient along the growth direction was observed. The composition was determined to be $(K_{0.47}Na_{0.53})(Nb_{0.72}Ta_{0.28})O_3$, $(K_{0.49}Na_{0.51})(Nb_{0.74}Ta_{0.26})O_3$, and $(K_{0.53}Na_{0.47})(Nb_{0.77}Ta_{0.23})O_3$ for the upper, middle, and bottom parts of the crystal. This composition gradient is a little lager than that of KNNT single crystal due to the larger radial dimension in the current case.[14] All samples used in this work were cut from the same slice of the crystal boule near the bottom.

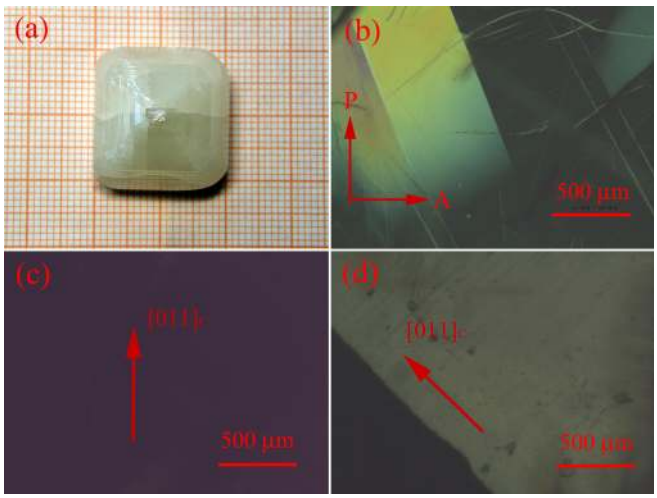

FIG. 1. (a) Photograph of as grown KNNT-2 single crystal; (b) domain configuration of the KNNT-2 single crystal before poling; (c) domain configuration of $[011]_C$ poled sample with $[011]_C$ parallel to the polarizer; and (d) domain configuration of $[011]_C$ poled sample with poling direction 45° to the polarizer.

Domain configurations of KNNT-2 single crystal before (Fig. 1(b)) and after (Figs. 1(c) and 1(d)) the two-step poling along $[011]_C$ were observed by PLM. All images are taken on the $[0\bar{1}1]_C$ surface. It can be seen from Fig. 1(b) that the domain width is of about 500 μm. After the two step poling, complete extinction was observed when the spontaneous polarization direction $[011]_C$ is parallel to one of the cross polarizers, as can be seen in Fig. 1(c). In Fig. 1(d), one can see that the whole sample is bright when $[011]_C$ is 45° to the polarizer. Combined from Figs. 1(c) and 1(d), it can be concluded that single domain state was achieved by the two-step poling process. The single domain state is proven rather unstable. Multidomain state can be easily induced by mechanical of electric stimuli. In fact, as the internal stress release gradually, domain walls were observed in all samples several days later. In some samples, domain walls can be observed at the edges of the sample immediately after the removal of poling electric field.

To determine the phase transition temperature of the KNNT-2 single crystal, temperature dependence of the dielectric constant ε_{33}^T for the $[011]_C$ poled sample was measured, and the results are presented in Fig. 2. The KNNT-2 single crystal exhibits two dielectric peaks in the measured temperature range. The peak around 85 °C corresponds to the orthorhombic-tetragonal phase transition temperature $T_{O\text{-}T}$ and the one at 253 °C corresponds to the tetragonal-cubic phase transition temperature T_C. Both T_C and $T_{O\text{-}T}$ are lower than that of the KNNT single crystal due to the higher Ta content in the current crystal.[14] The dielectric constant exhibits very little frequency dispersion and shows a sharp change near the Curie temperature T_C. Because the orthorhombic-tetragonal phase transition temperature $T_{O\text{-}T}$ is well above room temperature, pure orthorhombic phase is rather stable at room temperature, therefore, the properties are not very sensitive to the slight variation of composition and temperature, and self-consistent data sets can be expected.

The measured complete sets of elastic, piezoelectric, and dielectric constant for $[011]_C$ poled single domain KNNT-2 single crystal are listed in Table I. The single domain KNNT-2 crystal exhibits high transverse dielectric constant $\varepsilon_{22}^T = 1430$, much higher than the longitudinal dielectric constant $\varepsilon_{33}^T = 255$. On the other hand, the thickness shear piezoelectric coefficient d_{15} (251 pC/N) and d_{24} (166 pC/N) are 4.5

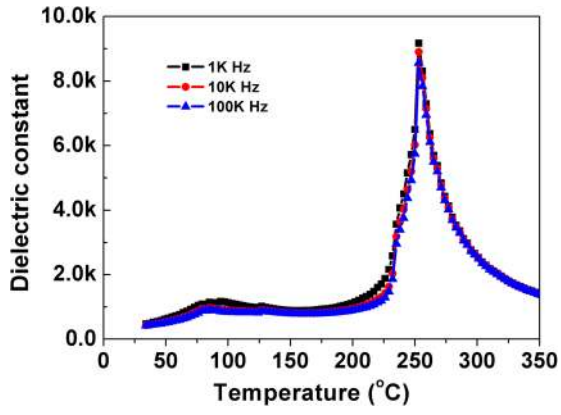

FIG. 2. Temperature dependence of the dielectric constant ε_{33}^T for the $[011]_C$ poled KNNT-2 single crystal.

TABLE I. Measured and derived material constants of $[011]_C$ poled single domain KNNT-2 single crystal. (Density: $\rho = 5165\,\text{kg/m}^3$).

Elastic stiffness constants: c_{ij}^E and c_{ij}^D ($10^{10}\,\text{N/m}^2$)

c_{11}^E	c_{12}^E	c_{13}^E	c_{22}^E	c_{23}^E	c_{33}^E	c_{44}^E	c_{55}^E	c_{66}^E
23.10	9.88	3.33	28.10	11.90	19.70	7.80	1.90	7.70
c_{11}^D	c_{12}^D	c_{13}^D	c_{22}^D	c_{23}^D	c_{33}^D	c_{44}^D	c_{55}^D	c_{66}^D
24.60	9.14	5.46	28.47	10.81	22.70	9.40	3.20	7.70

Elastic compliance constants: s_{ij}^E and s_{ij}^D ($10^{-12}\,\text{m}^2/\text{N}$)

s_{11}^E	s_{12}^E	s_{13}^E	s_{22}^E	s_{23}^E	s_{33}^E	s_{44}^E	s_{55}^E	s_{66}^E
5.11	−1.92	0.29	5.49	−2.99	6.83	12.82	52.63	12.99
s_{11}^D	s_{12}^D	s_{13}^D	s_{22}^D	s_{23}^D	s_{33}^D	s_{44}^D	s_{55}^D	s_{66}^D
4.66	−1.31	−0.50	4.65	−1.90	5.43	10.64	31.25	12.98

Piezoelectric coefficients: $d_{i\lambda}(10^{-12}\text{C/N})$, $e_{i\lambda}(\text{C/m}^2)$, $g_{i\lambda}(10^{-3}\,\text{Vm/N})$, $h_{i\lambda}(10^8\,\text{V/m})$

d_{15}	d_{24}	d_{31}	d_{32}	d_{33}	e_{15}	e_{24}	e_{31}	e_{32}	e_{33}
251	166	31.7	−43.5	56.2	4.76	12.96	4.90	−2.43	6.95
g_{15}	g_{24}	g_{31}	G_{32}	g_{33}	h_{15}	h_{24}	h_{31}	h_{32}	h_{33}
85.33	13.13	14.08	−19.31	24.93	27.30	12.34	30.59	−15.17	43.39

Dielectric constants: $\varepsilon_{ij}(\varepsilon_0)$ and $\beta_{ij}(10^{-4}/\varepsilon_0)$

ε_{11}^T	ε_{22}^T	ε_{33}^T	ε_{11}^S	ε_{22}^S	ε_{33}^S	β_{11}^T	β_{22}^T	β_{33}^T	β_{11}^S	β_{22}^S	β_{33}^S
332	1430	255	197	1187	181	30.14	6.99	39.27	50.76	8.42	55.25

Electromechanical coupling factors

k_{15}	K_{24}	k_{31}	k_{32}	k_{33}	k_t
0.637	0.412	0.296	0.391	0.453	0.365

times and 3 times as high as the longitudinal coefficient d_{33} (56.2 pC/N). Both dielectric and piezoelectric constants show very strong anisotropy, which is a typical characteristic of single domain crystals in the KNN systems.[23,24]

In order to calculate the orientation dependence of these physical properties, coordinate transformation has been performed on the single domain data sets. To describe the orientation dependence of dielectric, elastic, and piezoelectric properties, parameters of the single domain state in the intrinsic coordinate system are rotated counterclockwise first around the x-axis by an angle α, and then rotated counterclockwise around the new z'-axis by an angle γ in the 3-dimentional space. The transformed constants d_{33}*, s_{33}^E*, and ε_{33}^T* in the transformed coordinate system can be calculated using the data from the original matrices. The effective electromechanical coupling factor k_{33}* can be obtained by the following formula:

$$k_{33}{}^* = \frac{d_{33}{}^*}{\sqrt{\varepsilon_{33}^T{}^* s_{33}^E{}^*}}. \tag{1}$$

The corresponding parameters in the 3-dimensional space as functions of α and γ are shown in Fig. 3, where α increases in 3° steps and γ increases in 5° steps. From Fig. 3, it can be seen that d_{33}*, s_{33}^E*, ε_{33}^T*, and k_{33}* all show strong orientation dependence in the 3-dimentional space, d_{33}*, s_{33}^E*, and k_{33}* all reach their maximum values in the $(100)_C$ crystallographic plane. The transformed parameters d_{33}*, s_{33}^E*, ε_{33}^T* in the $(100)_C$ plane can be calculated by the following formulas:

$$d_{33}{}^* = (d_{31} + d_{15})\cos\beta\sin^2\beta + d_{33}\cos^3\beta, \tag{2a}$$

$$s_{33}^E{}^* = s_{33}^E\cos^4\beta + s_{11}^E\sin^4\beta + (2s_{13}^E + s_{55}^E)\cos^2\beta\sin^2\beta, \tag{2b}$$

$$\varepsilon_{33}^T{}^* = \varepsilon_{33}^T\cos^2\beta + \varepsilon_{11}^T\sin^2\beta, \tag{2c}$$

where β is the angle between $[011]_C$ and the new z'-axis. Material constants without asterisk (*) are corresponding parameters in the original coordinate system, and the constants with asterisk (*) are calculated data in the rotated coordinate system. k_{33}* is also obtained by Eq. (1). It can be concluded that when $\beta = 45°$, the z' axis is along $[001]_C$, corresponding to the $[001]_C$ poled domain engineered structure with 4 mm symmetry. As shown in Fig. 4, d_{33}* reaches its maximum value of 121.6 pC/N at $\beta = 50°$, while the highest $s_{33}^E{}^* = 16.3 \times 10^{-12}\,\text{m}^2/\text{N}$ and $k_{33}{}^* = 0.596$ are obtained at the angles of 45° and 54°, respectively. Dielectric constant ε_{33}^T* does not

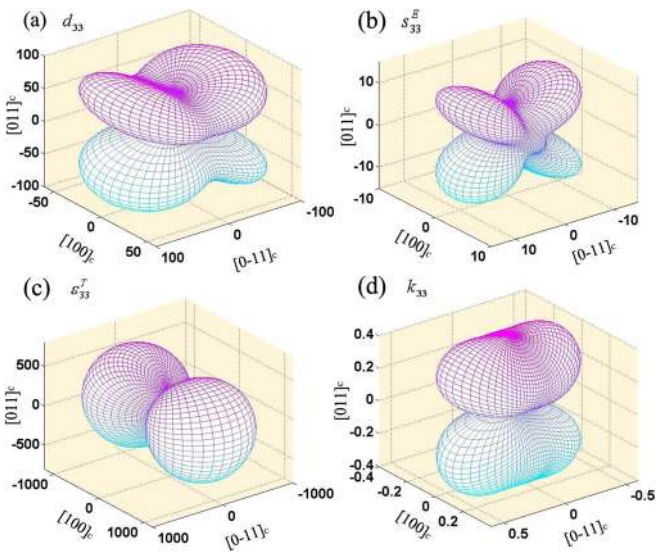

FIG. 3. Orientation dependence of (a) d_{33}*, (b) s_{33}^E*, (c) ε_{33}^T*, and (d) k_{33}* for the KNNT-2 single crystal.

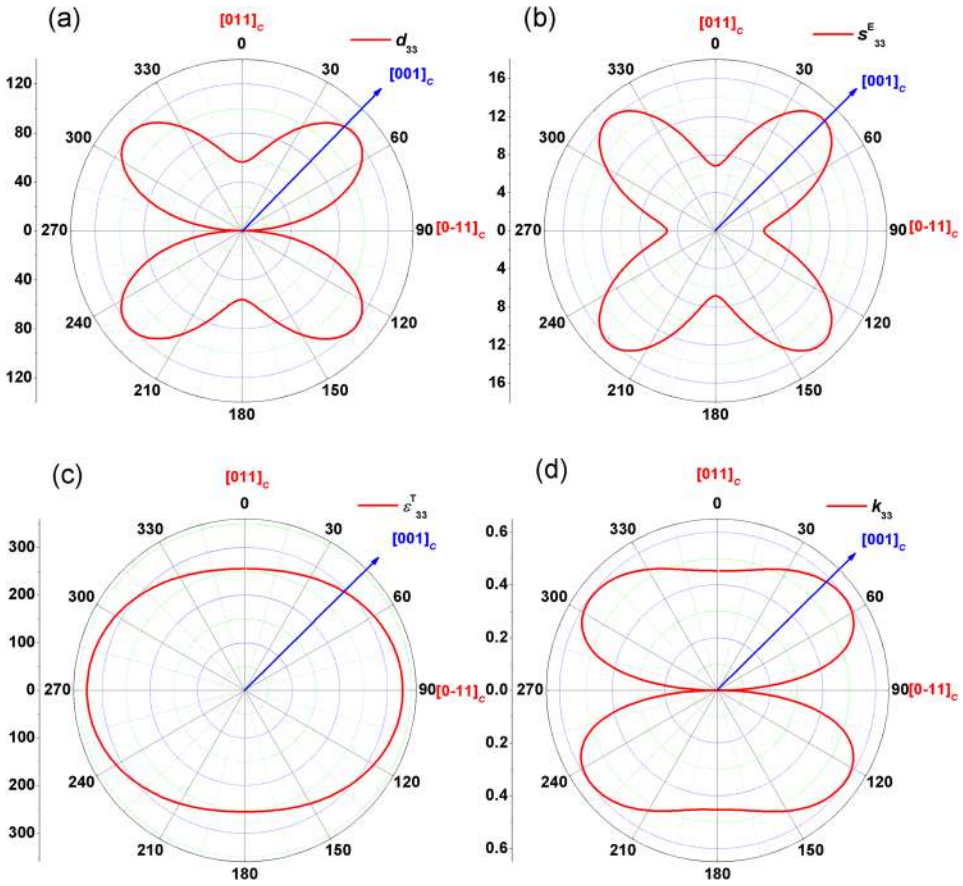

FIG. 4. Orientation dependence of (a) d_{33}*, (b) s_{33}^E*, (c) ε_{33}^T*, and (d) k_{33}* for the KNNT-2 single crystal in the $(100)_C$ crystallographic plane.

change as much as other constants with orientation in the $(100)_C$ plane due to the similar values of ε_{33}^T and ε_{11}^T in the single domain state. Although not all parameters reach the maximum value at 45°, all parameters exhibit near their corresponding maximum values along $[001]_C$.

The calculate values along $[001]_C$ are listed in Table II, and the corresponding material constants of $[001]_C$ poled domain engineered KNNT-2 single crystal with 4 mm symmetry are directly measured for comparison. It can be seen that the experimentally measured d_{33} is 150 pC/N, higher than the calculated value of 119.8 pC/N. This is because, in the calculated result based on the single domain data, no domain walls contribution were considered, only the intrinsic contribution from the effect of crystal anisotropy of a single-domain single crystal was taken into account. On the other hand, the experimental measured $[001]_C$ poled samples have multidomain structure, both intrinsic orientation effect and extrinsic domain wall contributions are included. The deviation between the calculated and measured values should be the extrinsic contributions, which are related to domain walls. We estimated that the extrinsic contribution is ~20%, higher than that of the relaxor $PbTiO_3$–based ferroelectric single crystals.[23,25] Previously, we had confirmed that the extrinsic contribution of $[001]_C$ poled Li, Ta modified KNN single crystals (determined by Rayleigh analysis method at the electric filed of 1 kV/cm) is 21.6%, very close to the calculated value here.[26] Furthermore, our previous work pointed out that the extrinsic contributions of the $[001]_C$ poled $0.95(Bi_{0.5}Na_{0.5})TiO_3$ based single crystal, determined by Rayleigh analysis, is ~10% at 1 kV/cm, which is also higher than that of the Pb-based relaxor single crystals, but lower than the KNN family.[27] So the extrinsic contributions, which are related to the domain wall activities, are related not only to domain configurations but also to specific material systems. The measured elastic compliance constant s_{33}^E is lower than the calculated value, indicating that the existence of domain walls hardened the material. The deviation between the calculated and measured k_{33} is relatively large, the reason cannot be explained by the current matrix transformation and needs to be further investigated.

TABLE II. Calculated and measured materials constants for $[001]_C$ poled KNNT-2 single crystal.

	d_{33} (pC/N)	s_{33}^E	ε_{33}^T	k_{33}
Calculated	119.8	16.3	293	0.582
Measured	150	12.7	273	0.820

In summary, a full set of elastic, dielectric, and piezoelectric constants for the $[011]_C$ poled single domain KNNT-2 crystal have been determined by the combined resonance, ultrasonic, and inverse impedance spectroscopy method. The single domain KNNT-2 crystal exhibits high anisotropy, with high shear piezoelectric coefficient ($d_{15} = 251$ pC/N, $d_{24} = 166$ pC/N) and low longitudinal piezoelectric coefficient ($d_{33} = 56.2$ pC/N). The orientation dependence of the longitudinal dielectric, piezoelectric, elastic, and electromechanical coupling properties were calculated based on the measured single domain full matrix data. It was found that the maximum $d_{33}^* = 121.6$ pC/N, $s_{33}^E{}^* = 16.3 \times 10^{-12}$ m^2/N, and $k_{33}^* = 0.596$ occur in the directions of 50°, 45°, and 54°, respectively, from the spontaneous polarization

direction in the $(100)_C$ plane. Near maximum d_{33}*, s_{33}^E, and k_{33}* values can be obtained in $[001]_C$ poled samples. By comparing calculated and experimental measured data for the $[001]_C$ oriented samples, the extrinsic piezoelectric contributions in the domain engineered single crystal is in the order of 20%, much larger than relaxor-$PbTiO_3$ based domain engineered crystals.

This work was supported by the National Key Basic Research Program of China (No. 2013CB632900), the National Natural Science Foundation of China (No. 51102062), the NIH under Grant No. P41-EB2182, the Fundamental Research Funds for the Central Universities (No. HIT. NSRIF. 2011011), and the Postdoctoral Foundation of Heilongjiang Province (No. LBH-Z10147).

[1]E. Hollenstein, M. Davis, D. Damjanovic, and N. Setter, Appl. Phys. Lett. **87**, 182905 (2005).
[2]J. Rödel, W. Jo, K. T. P. Seifert, E.-M. Anton, T. Granzow, and D. Damjanovic, J. Am. Ceram. Soc. **92**, 1153 (2009).
[3]K. Wang, F.-Z. Yao, W. Jo, D. Gobeljic, V. V. Shvartsman, D. C. Lupascu, J.-F. Li, and J. Rödel, Adv. Funct. Mater. **23**, 4079 (2013).
[4]L. Zheng, J. Wang, Q. Wu, G. Zang, C.-M. Wang, and J. Du, J. Alloys Compd. **487**, 231 (2009).
[5]S. Yasuyoshi, T. Hisaaki, H. Toshihiko, N. Tatsuhiko, T. Kazumasa, H. Takahiko, N. Toshiatsu, and N. Masaya, Nature **432**, 84 (2004).
[6]L.-Q. Cheng, K. Wang, and J.-F. Li, Chem. Commun. **49**, 4003 (2013).
[7]M. Morozov, H. Kungl, and M. Hoffmann, Appl. Phys. Lett. **98**, 132908 (2011).
[8]T. Shrout and S. Zhang, J. Electroceram. **19**, 113 (2007).
[9]K. Chen, G. Xu, D. Yang, X. Wang, and J. Li, J. Appl. Phys. **101**, 044103 (2007).
[10]J. G. Fisher, A. Benčan, M. Kosec, S. Vernay, and D. Rytz, J. Am. Ceram. Soc. **91**, 1503 (2008).
[11]Y. Inagaki, K.-I. Kakimoto, and I. Kagomiya, J. Eur. Ceram. Soc. **30**, 301 (2010).
[12]J. G. Fisher, A. Benčan, J. Holc, M. Kosec, S. Vernay, and D. Rytz, J. Cryst. Growth **303**, 487 (2007).
[13]Y. Inagaki and K. Kakimoto, Appl. Phys. Express **1**, 061602 (2008).
[14]L. Zheng, X. Huo, R. Wang, J. Wang, W. Jiang, and W. Cao, CrystEngComm **15**, 7718 (2013).
[15]G. Arlt and N. Pertsev, J. Appl. Phys. **70**, 2283 (1991).
[16]C. A. Randall, N. Kim, J.-P. Kucera, W. Cao, and T. R. Shrout, J. Am. Ceram. Soc. **81**, 677 (1998).
[17]Q. Zhang, H. Wang, N. Kim, and L. Cross, J. Appl. Phys. **75**, 454 (1994).
[18]S. Wada, A. Seike, and T. Tsurumi, Jpn. J. Appl. Phys., Part 1 **40**, 5690 (2001).
[19]E. Sun and W. Cao, Prog. Mater. Sci. **65**, 124 (2014).
[20]E. Sun, S. Zhang, J. Luo, T. R. Shrout, and W. Cao, Appl. Phys. Lett. **97**, 032902 (2010).
[21]S. Li, L. Zheng, W. Jiantg, R. Sahul, V. Gopalan, and W. Cao, J. Appl. Phys. **114**, 104505 (2013).
[22]S. Li, L. Zheng, and W. Cao, Appl. Phys. Lett. **105**, 012901 (2014).
[23]L. Zheng, R. Sahul, S. Zhang, W. Jiang, S. Li, and W. Cao, J. Appl. Phys. **114**, 104105 (2013).
[24]R. Zhang, B. Jiang, and W. Cao, Appl. Phys. Lett. **82**, 787 (2003).
[25]F. Li, S. Zhang, Z. Xu, X. Wei, J. Luo, and T. R. Shrout, J. Appl. Phys. **108**, 034106 (2010).
[26]X. Huo, L. Zheng, R. Zhang, R. Wang, J. Wang, S. Sang, Y. Wang, B. Yang, and W. Cao, CrystEngComm **16**, 9828 (2014).
[27]L. Zheng, X. Yi, S. Zhang, W. Jiang, B. Yang, R. Zhang, and W. Cao, Appl. Phys. Lett. **103**, 122905 (2013).